Observation of the $7^1\Pi_g$ State of Na_2 by Optical−Optical Double Resonance Spectroscopy

Chanchal Chaudhuri,[†] Ray-Yuan Chang,[†] Wei-Xiang Chen,[†] Wei-Chia Fang,[†] Jun-Ping Cheng,[‡] Thou-Jen Whang,[‡] and Chin-Chun Tsai*[,†]

Department of Physics, National Cheng-Kung University, Tainan 70101, Taiwan, and Department of Chemistry, National Cheng-Kung University, Tainan 70101, Taiwan

Received: April 18, 2007; In Final Form: June 21, 2007

The $7^1\Pi_g$ Rydberg state of Na_2 correlating with the separated atom limit Na(3s) + Na(5p) has been observed using high-resolution cw optical−optical double resonance spectroscopy. A total of 104 identified rovibrational levels in the range $v = 0-12$ and $11 \le J \le 44$ have been assigned to the $7^1\Pi_g$ state. Dunham coefficients were determined, and the Rydberg−Klein−Rees potential curve in the range of $R = 2.99-4.66$ Å was derived for the $7^1\Pi_g$ state using the observed quantum levels. The important molecular properties are the potential minimum $T_e = 36\,633.00(23)$ cm^{-1} at $R_e = 3.6313(29)$ Å, $\omega_e = 115.75(13)$ cm^{-1}, and $B_e = 0.111\,22(17)$ cm^{-1}. A detailed discussion of this investigation of the $7^1\Pi_g$ state is provided.

1. Introduction

The high monochromaticity of the laser coupled with powerful electronic devices has made it possible to observe rovibrational state-to-state selective transitions and enables one to identify unobserved electronic states. Alkali dimers have been frequently investigated both experimentally and theoretically with great interest because they have hydrogen-like simple electronic structure and transitions in the visible range. In particular, the Na_2 system has been studied for understanding different types of interactions playing important roles in diatomic molecules and to search for the answers to many intriguing questions about the fundamental physical properties of atoms and molecules. Researchers have carried out many works in investigating Na_2 using high level ab initio calculations[1,2] and experimental techniques[3−15] that involve many interesting and unusual features of the interactions.

Recently, a relabeling and classification of 84 Rydberg states with dissociation limits up to Na(3s) + Na(5p) have been reported by J. Li et al.[16] Neither of the *n*d-series ($^1\Pi_g$, $^1\Delta_g$) corresponding to Na(3s) + Na(*n*d) asymptotes has been investigated extensively. Using two-step polarization labeling spectroscopy, Carlson et al.[11] has reported five-parameter fit molecular constants (Dunham coefficients) of the *n*d $^1\Pi_g$-series ($n = 6 - 9$) in the range of $0 \le v \le 7$ and $19 \le J \le 41$, and the *n*d $^1\Delta_g$-series ($n = 6 - 12$) in the range of $0 \le v \le 3$ and $19 \le J \le 41$. They found that the estimated error of the fit was 0.3−0.4 cm^{-1}. Magnier et al.[1] calculated the potential curves of the states of Na_2 up to the separated atom limit of (3s + 5p). The state that is assigned to the $7^1\Pi_g$ state by them is assigned to the 6d $^1\Pi_g$ state by Carlson et al.[11] A high-resolution two-photon experimental technique "optical−optical double resonance" (OODR) spectroscopy is based on the simultaneous interaction between a molecule (or an atom) and two photons that are on resonance to two molecular (atomic) transitions involving certain energy levels. In this article, we report the OODR spectroscopic observation of the $7^1\Pi_g$ state, the molecular constants, and experimental Rydberg−Klein−Rees (RKR) potential curve of that state. A detailed discussion of the $7^1\Pi_g$ state is presented, and the effect of perturbations, if noticeable/significant or not, caused by the nearby states on this state is addressed.

2. Experimental Setup

The details of the optical−optical double resonance experimental setup with a block diagram can be found elsewhere.[12] Briefly, using the combination of ceramic-isolated heaters and Variacs, the sodium vapor is produced in a five-arm stainless steel heat-pipe oven. The temperature is maintained at 350 °C around its center and the pressure is at ∼1 Torr of argon buffer gas. To populate the intermediate $B^1\Pi_u$ state from the thermally populated ground state $X^1\Sigma_g^+$ of Na_2, a single line Ar^+ laser (Coherent I-90, total of nine lines; see Table-I of ref 10) is used. The Ar^+ laser is intensity-modulated at 1 kHz and counter-propagated to the single mode probe laser. Since the transitions of $X^1\Sigma_g^+ \rightarrow B^1\Pi_u$ have been intensively studied by Kusch and Hessel,[17] we calculate the term values of the populated $B^1\Pi_u$ levels from their Dunham coefficients (set III of Table 7 in ref 17) instead of adding the ground state term value to the laser frequency. Further, the details of the $X^1\Sigma_g^+ \rightarrow B^1\Pi_u$ transitions were reported by Camacho et al.[17] Single-mode tunable DCM (lasing range ∼14 300 cm^{-1}−16 500 cm^{-1}) and R6G (lasing range ∼16 400 cm^{-1}−17 700 cm^{-1}) ring-dye laser (Coherent 899-29 autoscan, pumped by a diode-pumped solid-state laser, Coherent Verdi-10) are used to probe the high-lying Rydberg states ($^1\Sigma_g^+$, $^1\Pi_g$, and $^1\Delta_g$) from the pumped intermediate rovibrational levels of the $B^1\Pi_u$ state.

The probed Rydberg states undergo collisional energy transfer and populate the adjacent triplet gerade states.[14,15] Subsequently, the UV fluorescence from these triplet gerade states to the $a^3\Sigma_u^+$ (3s + 3s) state is detected using a filtered photomultiplier tube (PMT) (filter: Sequoia-Turner Corp. 330−385 nm; photomultiplier tube, RCA84-22). The signals from the PMT are amplified by a lock-in amplifier (Stanford Research System SR-830) with the reference frequency of ∼1 kHz by chopping the Ar^+ laser beam. By scanning probe laser frequency, the signals of UV fluorescence from the PMT and the I_2 excitation spectrum

* Corresponding author. Fax: 886-6-2747995. E-mail: chintsai@mail.ncku.edu.tw.
† Department of Physics.
‡ Department of Chemistry.

10.1021/jp073002f CCC: $37.00
Published on Web 09/13/2007

(for frequency calibration) are simultaneously recorded by autoscan software and displayed on a personal computer.[19] The line positions of our OODR spectra can be determined to within 0.02 cm^{-1}. The uncertainty is mainly due to pumping the thermally populated ground state molecules by a frequency-fixed Ar^+ laser line and the laser power broadening. The molecules with thermal velocity may be pumped off-resonance due to the Doppler effect, which causes a shift in the line center. For the transitions $X^1\Sigma_g^+ \rightarrow B^1\Pi_u$ (v', J') by a single line Ar^+ laser, the estimated off-resonance uncertainty due to the Doppler shift (could be red- or blue-detuned, T_{vj} [$B^1\Pi_u$ (v', J')] − (T_{vj}[$X^1\Sigma_g^+$ (v'', J'')] + $h\nu_{probe}$), where $h\nu_{probe}$ is the single line Ar^+-laser resonance energy) ranges from 0.017 cm^{-1} to 0.149 cm^{-1} for the observed levels in the present work. So the total maximum experimental uncertainty in measuring the OODR-line positions (including the off-resonance uncertainty) of the probed excited state can be 0.169 cm^{-1}.

3. Results and Analysis

The experiment was carried out to record the nine sets of OODR spectroscopic data of the intensities versus wavenumbers of the excitation fluorescence signals for the rovibrational transition processes, $X^1\Sigma_g^+ \rightarrow B^1\Pi_u \rightarrow {}^1\Sigma_g^+$, $^1\Pi_g$, $^1\Delta_g$, guided by the selection rules $\Delta\Lambda = 0, \pm1$; $\Delta S = 0$; $\Delta J = 0, \pm1$, and $g \nleftrightarrow u$,[20] corresponding to each single line of nine Ar^+ pump laser lines. The detailed studies of Kusch et al.[17] and Camacho et al.[18] provided extensive information about the transitions from the $X^1\Sigma_g^+$ state to the $B^1\Pi_u$ state. From our OODR recorded spectra, two kinds of many obvious vibrational progressions of the patterns consisting of (P, Q, R) and (P, R) lines of different electronic states have been identified. Taylor et al.[21] pointed out that the signals from the transitions between $B^1\Pi_u$ and $^1\Sigma_g^+$ rovibrational states are weak. So the observed signals in an OODR experiment would primarily be related to the $^1\Pi_g$ and $^1\Delta_g$ states. The study by Pan et al.[22] indicated to us the transitions from rovibrational $B^1\Pi_u$ states to $^1\Delta_g$ states show a strong Q line accompanied by two half-intensity P, R lines for each upper v level, whereas the transitions from rovibrational $B^1\Pi_u$ states to $^1\Pi_g$ states show only strong P, R lines with an extremely weak or absent Q line. So the observed vibrational progressions with the pattern consisting of only P and R rotational lines are due to the $B^1\Pi_u \rightarrow {}^1\Pi_g$ rovibrational transitions.

To analyze the data, first we assign the rotational quantum number J of the observed progressions in the recorded spectra. The energy difference between the P and R lines $T(v, J+1) - T(v, J-1) \approx 4Y_{01}(J + 1/2)$ is approximately proportional to J. This leads to a tentative assignment of the rotational quantum numbers J of the intermediate levels and that of the probed excited levels. In addition, in the progressions, we can readily determine the term values of the progressions from the relation $T(v, J/J \pm 1) \approx T_{B^1\Pi_u}(v', J) + h\nu_{probe}$. The term value expression of the Dunham double power series to the lowest order is given by

$$T(v, J) \cong T_e + \omega_e\left(v + \frac{1}{2}\right) + B_e[J(J+1) - \Lambda^2] \qquad (1)$$

Now, if the assigned (P, R) lines of the v progressions are plotted as $T(v, J)$ vs $[J(J+1) - \Lambda^2]$, the data points belonging to the same v values of a single electronic state give unique straight lines. From a huge number of tentatively assigned lines (~1100) of $^1\Pi_g$ character (P, R branches) of the probed states in the nine sets of spectra, we have sorted out correct v progressions belonging to individual $^1\Pi_g$ electronic states. An idea of the potential minimum, T_e (theoretical/experimental),

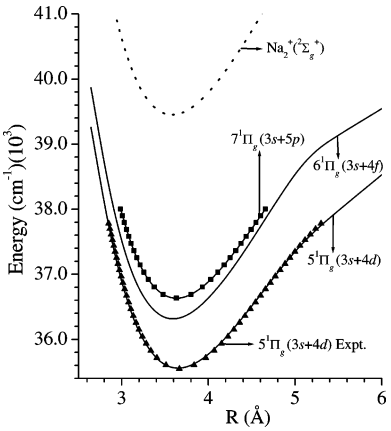

Figure 1. Experimental RKR potential curve of the $7^1\Pi_g$ state in the observed range of $v = 0-12$ (solid squares connected by a solid line) together with the $5^1\Pi_g$ (experiment, solid triangles; calculation, solid line), $6^1\Pi_g$ (calculation, solid line), and Na_2^+ $^2\Sigma_g^+$ (Na^+ + Na(3s)) (calculation, dotted line). All calculated potential curves are elevated by ~230 cm^{-1} scaled with the experimental $5^1\Pi_g$ potential curve for close comparisons.

is certainly helpful to look for the potential minimum or the region in its vicinity of a particular state in the observed data ($T(v, J)$ vs. $[J(J+1) - \Lambda^2]$ plot) and the assignment. For instance, the value of T_e is 36 634.01 cm^{-1} for the $6d^1\Pi_g$ state in Carlson's work.[11]

We have started with a set of ~200 data points (tentatively assigned J values to the PR lines) in the $T(v, J)$ vs $[J(J+1) - \Lambda^2]$ plot. This plot also helps as a tool to predict the progressions that have not been picked out or are missing, rather than only as an initial checking of the J assignments. The second step is to assign the vibrational quantum numbers, v, and we assign the observed lowest vibrational level to $v = 0$ (Supporting Information Figure 1). After v, J assignments (tentatively), we run the programs to do Dunham fitting by the least-square fitting algorithm to obtain the Dunham coefficients that are represented by Dunham double power series expansion as follows,

$$T_{v,J} = \sum_{i,j} Y_{ij}\left(v + \frac{1}{2}\right)^i [J(J+1) - \Lambda^2]^j \qquad (2)$$

where Y_{ij} are the Dunham coefficients and $\Lambda = 1$ for Π states. Starting with a five-parameter Dunham fit, eventually we have optimized to an eight-parameter Dunham fit using the picked up lines from the recorded spectra. Separating the e/f-parity levels in the Dunham run, the discrepancy (O−C), which is the difference between the observed energy and the calculated energy from the Dunham polynomial fit, is preset to 0.7 cm^{-1} (optimized) to obtain a standard deviation of 0.154 cm^{-1} (nearly equal to the total experimental uncertainty of 0.169 cm^{-1}). In the Dunham fit output file (Supporting Information), if O−C of any one line of an e-parity PR pair is over the preset value of 0.7 cm^{-1}, that PR pair is a "deviant PR pair", and the rest are the "nondeviant PR pairs" in our Dunham fit. Excluding the deviant PR pairs of the data set in the Dunham fit, 94 rovibrational e-levels and 10 f-levels have been identified and assigned to the vibrational and rotational quantum numbers in the range of $v = 0-12$ and $11 \leq J \leq 44$, respectively. In the Supporting Information, we displayed the plot of the term values, $T(v, J)$, of these progressions against $[J(J+1) - \Lambda^2]$ in the regime of $v = 0 - 12$ and $11 \leq J \leq 44$, in which the data points corresponding to the same vibrational quantum number v are linear (excluding deviant PR pair data points in the Dunham fit). The observed term values and those calculated

TABLE 1: Rovibrational Molecular Transitions from the Intermediate $B^1\Pi_u$ State to the $7^1\Pi_g$ State in Na_2 Corresponding to the Different Single Line Ar^+ Laser to Pump from the $X^1\Sigma_g^+$ Ground State (All e-Parity Levels) to the $B^1\Pi_u$ State Observed in the Present Work[a]

Ar^+ laser($^1\Sigma_g^+$) (nm) (v'', J'')	$B^1\Pi_u$ (v', J')	$7^1\Pi_g$ (v, $J = J' \pm 1$)
	e-Parity	
472.7 (1, 37)	(9, 38)	($v = 5-11$)
476.5 (0, 28)	(6, 27)	($v = 2-8$, $10-12$)
476.5 (3, 13)	(10, 12)	($v = 6-9$, 12)
496.5 (7, 29)	(8, 28)	($v = 4-7$, 9)
496.5 (6, 44)	(7, 43)	($v = 3-6$, 8, 9, 11, 12)
501.7 (2, 43)	(0, 42)	($v = 0-3$)
501.7 (6, 38)	(5, 37)	($v = 2$, 3, $9-11$)
488.0 (6, 41)	(10, 42)	($v = 6-8$)
	f-Parity	
488.0 (3, 43)	(6, 43)	($v = 2-5$, 7)

[a] Comparing the matching between the global Dunham fit and the FCFs calculated between the $B^1\Pi_u$ and $7^1\Pi_g$ states. Camacho et al.[18] reported details of the $X^1\Sigma^+_g \rightarrow B^1\Pi_u$ transitions.

from the molecular constants and differences between them are listed in the Supporting Information. This confirms that all these nondeviant assignments of J of the intermediate energy level out of the tentatively assigned J-values for PR-lines in the raw spectra are correct, that is, they belong to the same electronic state. In addition, it is quite evident from this plot that all the data points belong to a single progression excited from the same level of the intermediate $B^1\Pi_u$ state. The rovibrational levels of the observed state are excited from the intermediate $B^1\Pi_u$-[(v', J') = (0, 42), (5, 37), (6, 27), (7, 43), (8, 28), (9, 38), (10, 12), (10, 42), and (6, 43)] rovibrational levels (Supporting Information).

Using the eight-parameter set of Dunham coefficients, we have constructed a rotationless Rydberg−Klein−Rees potential within the restricted range of $v = 0-12$ and calculated the Franck−Condon factors (FCFs) between the energy levels of the $B^1\Pi_u$ state and the observed $^1\Pi_g$ state. The FCFs compare well with the observed normalized intensities of the P, R lines for each vibrational progression and will be addressed in the next section. The minimum of the RKR potential curve (T_e = 36 633.00 cm^{-1}) agrees well with the experimental result by Carlson et al.[11] (less by 1 cm^{-1}), and they assigned this to the $6d^1\Pi_g$ state. Calculation by Magnier et al.[1] shows that the value of T_e = 36 337 cm^{-1} (lower by 296 cm^{-1} than our result) is assigned to the $7^1\Pi_g$ state. Notably, the calculated values of T_e of the states of Na_2 by Magnier et al.[1] (by method B) are lower by ∼200−300 cm^{-1} than experimental T_e values. So following Magnier et al.,[1] we assign our observed state to the $7^1\Pi_g$ state, which goes to the separated atom limit of Na(3s) + Na(5p). Table 1 lists the rovibrational transitions $X^1\Sigma_g^+$ (v'', J'') → $B^1\Pi_u$ (v', J') → $7^1\Pi_g$ (v, $J = J' \pm 1$), corresponding to the different single line Ar^+ pump laser observed in this work.

To minimize the error in the data fits, the Λ-doubling that manifests itself in the splitting of the e/f parity levels has been considered in the present work. For electric-dipole transitions, the selection rules for allowed transitions are e ↔ e, f ↔ f for both the P and R branches and e ↔ f for the Q branch. In the data set of the $7^1\Pi_g$ state, we have found only 10 f-parity levels ($v = 2-5$, 7; $J = 42$, 44) out of a total of 104 P, R lines. From the eight-parameter Dunham fit, we have estimated the discrepancy δ_{f-e}, which is the difference between the observed term value of f-parity levels and the calculated term value from Dunham coefficients Y_{ij} of the e-parity levels using the same set of rovibrational quantum numbers (v, J). The discrepancy δ_{f-e} is a measure of the Λ-doubling quantitatively, but not a precise one. The dependence of δ_{f-e} on the vibrational quantum number (v + 1/2) is almost constant (−0.495 ± 0.075 cm^{-1}), and only that on rotational quantum numbers $J = 42$ and 44 cannot provide any information over a wide range of J for the $7^1\Pi_g$ state. Furthermore, to have an idea about the values of the Λ-doubling splitting constants (q_0, q_v, and μ), all 10 δ_{f-e} values were three-parameter Dunham least-square-fitted to generate three Dunham coefficients that are related to the Λ-doubling energy term ($T_{\lambda d}$) through the following modified Dunham expression,

$$T_{v,J} = \sum_{i,j} Y_{ij}\left(v + \frac{1}{2}\right)^i [J(J+1) - \Lambda^2]^j + \delta[J(J+1) - \Lambda^2]\left\{q_0 + q_v\left(v + \frac{1}{2}\right) + \mu[J(J+1) - \Lambda^2]\right\} \quad (3)$$

where the whole term multiplied by δ is $T_{\lambda d}$. $\delta = 0$ for e-parity levels and $\delta = -1$ for f-parity levels. The derived Dunham coefficients (Y_{ij}) of the $7^1\Pi_g$ state are listed in Table 2 (with e-parity levels only). Y_{00} and the other four Y_{ij}s compare well with Carlson's data.[11] The Λ-doubling splitting constants estimated from 10 levels of f-parity are $q_0 = 0.4120 \times 10^{-3}$, $q_v = -0.7312 \times 10^{-5}$, and $\mu = -0.5937 \times 10^{-7}$. For eq 3, the significant contribution of q_0 depends only on $[J(J+1) - \Lambda^2]$, whereas that of q_v comes from both $[J(J+1) - \Lambda^2]$ and (v + 1/2), and that of μ depends on the square of $[J(J+1) - \Lambda^2]$. But due to the lack of a wide range of v, J for the f-level data set (only 10, $v = 2 - 5,7$; $J = 42$, 44), the quantitative values of q_0, q_v and μ are not statistically so meaningful, particularly the value of μ (so not listed in Table 2); however, the evidence of the Λ-doubling of the rovibrational levels of the $7^1\Pi_g$ state is clear from the δ_{f-e} values, as mentioned above. A detailed discussion of this state is as follows.

4. Discussion

For the $7^1\Pi_g$ state, a total of 104 rovibrational levels were identified and assigned to the vibrational and rotational quantum numbers in the range of $0 \le v \le 12$ and $11 \le J \le 44$, respectively. Carlson et al.[11] reported their determination of the set of five Dunham coefficients of this state in the range of $0 \le v \le 7$ and $19 \le J \le 41$, with an estimated error of the fit of 0.35 ± 0.05 cm^{-1}. The important molecular constants are compared with those of Carlson's work in Table 2. The values of the Dunham coefficients (eq 2) depend on the range of v and J as well as the number of coefficients included for Dunham fitting. The value of T_e in their work is ∼1 cm^{-1} higher than our experimental result. The value of ω_e (115.75 cm^{-1}) differs by only 0.18 cm^{-1}. As seen in Table 2, the determined value and its deviation (uncertainty) of the molecular constant Y_{30} are 0.115 10 × 10^{-2} cm^{-1} and 0.39 × 10^{-2} cm^{-1}, respectively, and those of the molecular constant Y_{40} are −0.175 17 × 10^{-3} cm^{-1} and 0.14 × 10^{-3} cm^{-1}, respectively. For Y_{30}, the deviation is even higher than the absolute value, and for Y_{40}, the deviation is almost the same as the absolute value. This implies that there is a limit, that is, the maximum number of the Dunhum coefficients taken in the Dunham fit (eight-parameter), for the $7^1\Pi_g$ state in this work, which is due to the lack of a wide range of the observed data field. Note that these values depend on the rotational levels of the lowest vibrational state.

Table 3 (see also Figure 2 in the Supporting Information) displays the observed separations between the successive vibrational levels $\Delta G_{v+1/2}$ (= $G(v+1) - G(v)$). This shows a

TABLE 2: Molecular Constants (cm^{-1}) from the Present Experimental Results[a]

Y_{ij}	this work	Carlson et al.[10]	Magnier et al.[1]
Y_{00}	$0.366\,330\,0 \times 10^5$ (0.23×10^0)	$0.366\,340\,1 \times 10^5$ (0.1×10^0)	$0.363\,37 \times 10^5$
Y_{10}	$0.115\,745 \times 10^3$ (0.13×10^0)	$0.115\,560 \times 10^3$ (0.1×10^0)	$0.113\,7 \times 10^3$
Y_{20}	$-0.487\,002 \times 10^0$ (0.36×10^{-1})	$-0.474\,6 \times 10^0$ (0.1×10^{-1})	
Y_{30}	$0.115\,10 \times 10^{-2}$ (0.39×10^{-2})		
Y_{40}	$-0.175\,17 \times 10^{-3}$ (0.14×10^{-3})		
Y_{01}	$0.111\,215\,7 \times 10^0$ (0.17×10^{-3})	$0.109\,39 \times 10^0$ (0.1×10^{-3})	
Y_{11}	$-0.694\,94 \times 10^{-3}$ (0.10×10^{-4})	-0.601×10^{-3} (0.4×10^{-4})	
Y_{02}	$-0.407\,2 \times 10^{-6}$ (0.58×10^{-7})		
σ	$0.154\,030\,65 \times 10^0$		

[a] Carlson's work[11] and Magnier's work[1] for the $7^1\Pi_g$ state of Na_2 are listed. The seemingly superfluous digits are necessary to compensate for the eects of correlations between the constants. σ is the standard deviation of the global Dunham fit.

TABLE 3: RKR Potential Curve of the $7^1\Pi_g$ State of Na_2[a]

v	B_v (cm^{-1})	$G_v + Y_{00}$ (cm^{-1})	$\Delta G_{v+1/2}$ (cm^{-1})	R_{min} (Å)	R_{max} (Å)
0	0.110 87	57.750	114.774	3.4791	3.7981
1	0.110 17	172.524	113.806	3.3760	3.9305
2	0.109 48	286.330	112.835	3.3089	4.0271
3	0.108 78	399.165	111.859	3.2565	4.1093
4	0.108 09	511.025	110.874	3.2126	4.1832
5	0.107 39	621.899	109.874	3.1745	4.2515
6	0.106 70	731.772	108.855	3.1406	4.3158
7	0.106 00	840.628	107.815	3.1100	4.3772
8	0.105 31	948.442	106.747	3.0819	4.4363
9	0.104 61	1055.189	105.649	3.0559	4.4935
10	0.103 92	1160.838	104.515	3.0316	4.5494
11	0.103 22	1265.353	103.342	3.0087	4.6042
12	0.102 53	1368.695		2.9871	4.6581

[a] The second order correction to the zero point energy is $Y_{00} = -0.001\,013$ cm^{-1}, and the equilibrium position is $R_e = 3.6313$Å, whereas in Magnier's work[1] $R_e = 3.5983$Å.

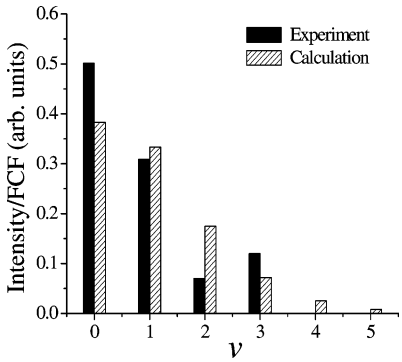

Figure 2. Comparison of the intensities (normalized) of the observed PR lines with the calculated FCFs between the $B^1\Pi_u$ and $7^1\Pi_g$ states excited from $B^1\Pi_u$ (0, 42).

linear part ($v = 0-6$) with a slow decrease afterward ($v = 7-12$) and a very regular behavior of the successive vibrational levels in an anharmonic potential well within the observed range of $v = 0-12$. Table 3 (Figure 3 in the Supporting Information, as well) represents a quite linear dependence of the rotational constants, B_v, with v ($= 0-12$). The B_v value decreases by about 0.008 33 cm^{-1} when v increases from 0 to 12, that is, B_v decreases by 0.000 695 cm^{-1} per unit change of v. Dunham-fitted Y_{ij} data (Table 2) were used to construct the RKR potential of the $7^1\Pi_g$ (3s + 5p) state shown in Figure 1, together with potential curves of the $5^1\Pi_g$ (3s + 4d) state,[13,1] $6^1\Pi_g$ (3s + 4f) state,[1] and the $^2\Sigma_g^+$ ground state of Na_2^+,[1] to have a pictorial view of the closeness among them. All the calculated potential curves are elevated by ~230 cm^{-1} scaled with the experimental $5^1\Pi_g$ potential curve for close comparisons. Table 3 lists the data set for the RKR potentials of the $7^1\Pi_g$ state in Na_2. We have identified transitions from $v' = 0$, 5−10 of the $B^1\Pi_u$ state to $v = 0-12$ of the $7^1\Pi_g$ state. The FCFs (Supporting Information) between the $7^1\Pi_g$ and the $B^1\Pi_u$ states were calculated to compare with the observed normalized intensities, and a reasonable agreement was found. The observed line intensities were normalized and scaled if the dye was changed (DCM to R6G) to scan a higher range, and the laser power was almost constant (it was not effective to vary the signal intensities) over the scanned range with a single type of dye. In addition, we assume that the equivalent collisional energy transfer occurs from the $7^1\Pi_g$ state to the upper triplet gerade states involved (also an equal priority probability for a random process) which subsequently fluoresce to the $a^3\Sigma_u^+$ state,[14,15] and we assume that the electronic transition dipole moments are approximately invariant over the observed range of internuclear distance (R). The FCF table and the Dunham output (Supporting Information) show that the trend of the distributions of excitation probability among the different v-levels of the excited $7^1\Pi_g$ state compare quite well with each other. Figure 2 illustrates the similarity between the trends of the observed transition probabilities (normalized intensities of the observed v-progressions of the $7^1\Pi_g$ state) and the calculated transition probabilities (FCFs between the $B^1\Pi_u$ and $7^1\Pi_g$ states excited from v', $J' = 0$, 42 to $v = 0-12$), the intensities die out at $v = 4$ and 5, respectively. In addition, the oscillating probabilities are clear both in the Dunham output and the FCF Table (Supporting Information), and they are in good agreement, as well (for instance, the transitions excited from $v'J' = (5, 37)$ and (6, 27)). All these good agreements in turn confirm that both the v and the J assignments of the rovibrational levels of the observed electronic state $7^1\Pi_g$ are correct.

Figure 1 illustrates the experimental RKR potential of the $7^1\Pi_g$ state with $T_e = 36\,633.00$ cm^{-1} at $R_e = 3.6313$ Å. Combined with the smooth and regular anhamonicity of the potential curve as it appears in the presence of the $5^1\Pi_g$, $6^1\Pi_g$, and Na^+ $^2\Sigma_g^+$ states, the linearity and the regular pattern of both $\Delta G_{v+1/2}$ with $v + 1/2$ (Supporting Information) and B_v with v (Supporting Information), and the good agreement between the observed normalized intensities and the calculated FCFs suggest that there is no effect of noticeable or significant perturbations produced by other nearby electronic states on the $7^1\Pi_g$ state. The total molecular wavefunction can be represented by the linear combination of the atomic orbitals of the individual atoms in the Na_2 dimer, that is, $\psi_{7^1\Pi_g} = \phi_{3s} + \phi_{5p}$, where ϕ_{3s} and ϕ_{5p} are the atomic wavefunctions of the 3s and 5p orbitals, respectively. The transition probabilities calculated using the electric dipole transition moment (assuming invariant over R) between the $7^1\Pi_g$ state and the $B^1\Pi_u$ state (or any similar type of state) will be qualitatively good and could be reasonable in quantitative accuracy, as well.

5. Conclusions

In this work, we have derived Dunham coefficients and constructed the rotationless RKR potential of the $7^1\Pi_g$ state from

the observed rovibrational quantum levels. Although obvious Λ-doubling is observed ($\delta_{f-e} = -0.495 \pm 0.075$ cm^{-1} obtained from $v = 2-5, 7$; $J = 42, 44$), the Λ-doubling splitting constants (q_0, q_v, and μ) are not quantitatively so meaningful from a statistical point of view due to a lack of a wide range of observed f-level data. Within the total experimental uncertainty (0.169 cm^{-1}) of the line position and the standard deviation of Dunham fit (0.154 cm^{-1}) of the observed data, this detailed investigation suggests that the $7^1\Pi_g$ state does not show up any noticeable signature of perturbations caused by the neighboring states in the observed range of $R = 2.99-4.66$ Å of Na_2. Due to the absence of a significant effect of the perturbations produced by nearby states, it seems that for simplicity, the $7^1\Pi_g$ state could be treated as an unperturbed state of Na_2. This observation of the $7^1\Pi_g$ state in the Na_2 system would draw the attention of researchers to investigate the higher Rydberg states of Na_2 and other alkali dimers and shed light on interactions in diatomic molecules.

Acknowledgment. We gratefully acknowledge the support of this work by the National Science Council, Taiwan.

Supporting Information Available: (1) Figure 1: the term values $T(v, J)$ vs. $[J(J + 1) - \Lambda^2]$ plot in the regime of $v = 0-12$ and $11 \leq J \leq 44$ excluding the deviant PR lines in the Dunham fit. (2) The Dunham fit output (with e-parity levels only) for the observed rovibrational levels of the $7^1\Pi_g$ state. v, vibrational quantum number; J, rotational quantum number; OBS, term values from the experimental observations; CALC, term values calculated from the Dunham fit molecular constants (Y_{ij}); and O − C, the difference between the OBS and CALC. All the units of the energy levels are in cm^{-1}. (3) Figure 2: Separations between the successive vibrational levels ($\Delta G_{v+1/2}$) versus ($v + 1/2$) for the observed $7^1\Pi_g$ state. Data points (full squares) are joined by a solid line to guide the eye. The assigned lowest vibrational level is $v = 0$. (4) Figure 3: The rotational constant, B_v, as a function of vibrational quantum number, v, for the observed $7^1\Pi_g$ state. Data points (solid squares) are joined by a solid line to guide the eye. (5) Franck−Condon factors table between the $B^1\Pi_u$ and the $7^1\Pi_g$ states in the Na_2 system. This material is available free of charge via the Internet at http://pubs.acs.org.

References and Notes

(1) Magnier, S.; Milliè, Ph.; Dulieu, O.; Masnou-Seeuws, F. *J. Chem. Phys.* **1993**, *98*, 7113.
(2) Magnier, S. Ph. D. Thesis, Universie De Paris-Sud, Centre D'orsay, 1993.
(3) Knöckel, H.; Johr, T.; Richter, H.; Tiemann, E. *Chem. Phys.* **1991**, *152*, 399.
(4) Wang, H.; Whang, T. J.; Lyyra, A. M.; Li, L.; Stwalley, W. C. *J. Chem. Phys.* **1991**, *94*, 4756.
(5) Tsai, C. C.; Bahns, J. T.; Whang, T. J.; Wang, H.; Stwalley, W. C.; Lyyra, A. M. *Phys. Rev. Lett.* **1993**, *71*, 1152.
(6) Cooper, D. L.; Barrow, R. F.; Vergès, J.; Effantin, C.; D'Incan, J. *Can. J. Phys.* **1984**, *62*, 1543.
(7) Ratliff, L. P.; Wagshul, M. E.; Lett, P. D.; Rolston, S. L.; Phillips, W. D. *J. Chem. Phys.* **1994**, *101*, 2638.
(8) Tsai, C. C.; Bahns, J. T.; Stwalley, W. C. *J. Chem. Phys.* **1993**, *99*, 7417.
(9) Barrow, R. F.; Amiot, C.; Vergès, J.; d'Incan, J.; Effantin, C.; Bernard, A. *Chem. Phys. Lett.* **1991**, *183*, 94.
(10) Chang, R. Y.; Tsai, C. C.; Whang, T. J.; Cheng, C. P. *J. Chem. Phys.* **2005**, *123*, 224303.
(11) Carlson, N. W.; Taylor, A. J.; Jones, K. M.; Schawlow, A. L. *Phys. Rev. A: At., Mol., Opt. Phys.* **1981**, *24*, 822. Carlson, N. W.; Taylor, A. J.; Schawlow, A. L. *Phys. Rev. Lett.* **1980**, *45*, 18.
(12) Whang, T. J.; Wu, H. W.; Chang, R. Y.; Tsai, C. C. *J. Chem. Phys.* **2004**, *121*, 010513.
(13) Tsai, C. C.; Chang, R. Y.; Whang, T. J. *J. Mol. Spectrosc.* **2005**, *234*, 264.
(14) Li, L.; Field, R. W. *J. Mol. Spectrosc.* **1986**, *117*, 245.
(15) Pichler, G.; Bahns, J. T.; Sando, K. M.; Stwalley, W. C.; Konowalow, D. D.; Li, L.; Field, R. W.; Muller, W. *Chem. Phys. Lett.* **1986**, *129*, 425.
(16) Li, J.; Liu, Y.; Dai, X.; Li, L.; Field, R. W. *J. Chem. Phys.* **2001**, *114*, 7859.
(17) Kusch, P.; Hessel, M. M. *J. Chem. Phys.* **1978**, *68*, 2591.
(18) Camacho, J. J.; Pardo, A.; Poyato, J. M. L. *J. Phys. B* **2005**, *38*, 1935.
(19) *Coherence Autoscan Operator's Manual*, PC Verson; Coherent, Inc.: Santa Clara, California 1994; Part No. 0162-80600.
(20) Herzberg, G. *Molecular Spectra and Molecular Structure I. Spectra of Diatomic Molecules*, 2nd ed.; Krieger Publishing Co.: Malabar, Florida, 1989.
(21) Taylor, A. J.; Jones, K. M.; Schawlow, A. L. *J. Opt. Soc. Am.* **1983**, *73*, 994.
(22) Pan, Y. L.; Ma, L. S.; Ding, L. E.; Sun, D. P. *J. Mol. Spectrosc.* **1993**, *162*, 178.